

RESEARCH LETTER

Iron Inhibits the Secretion of Apolipoprotein E in Cultured Human Adipocytes



Nonalcoholic steatohepatitis (NASH) is characterized by adipose tissue dysfunction with insulin resistance and the dysregulation of adipokines.¹ Recent data indicate repartitioning of iron from the liver to adipocytes in obesity and a role for iron in the development of adipose tissue dysfunction.^{2,3} However, the molecular mechanisms have not been established. To test the hypothesis that iron modulates adipokine release, we performed a quantitative proteomics analysis of the human Simpson-Golabi-Behmel Syndrome (SGBS) adipocyte secretome after 48 hours of treatment with ferric ammonium citrate (FAC). We used stable isotope-labeled amino acids in cell culture (SILAC) to characterize changes in the adipocyte secretome in response to iron. This technique has enabled direct comparison of quantities of individual proteins in the adipocyte secretome in response to iron using a proteomics approach as a tool for the identification of novel treatment targets in NASH. Detailed methodology is described in [Supplementary Methods](#).

We first showed that 100 $\mu\text{mol/L}$ FAC causes significant adipocyte iron

loading without compromising cell viability. We found that compared with vehicle, both 100 $\mu\text{mol/L}$ and 500 $\mu\text{mol/L}$ FAC caused significant increases in cellular iron concentration ($P = .007$ and $P = .006$, respectively) ([Supplementary Figure 1A](#)). There was no effect of iron loading on cellular viability (MTS) assay, total messenger RNA (mRNA), total whole-cell lysate protein, or total secretome protein ([Supplementary Figure 1B–E](#)).

Given these findings, we selected 100 $\mu\text{mol/L}$ FAC as the concentration to compare with vehicle in the secretome SILAC proteomic analysis. A total of 338 proteins were quantified in the adipocyte secretome by SILAC proteomics. These are represented by the volcano plot in [Supplementary Figure 2](#) and the proteomics data have been deposited into the ProteomeXchange Consortium via the Proteomics Identifications (PRIDE) partner repository (www.proteomexchange.org) with the data set identifier PXD006341. Iron treatment led to significant differential secretion of 60 of these proteins (>2 -fold change; $P < .05$). We then manually reviewed UniProt database descriptions of these 60 proteins.⁴ This generated a list of 20 proteins of interest (highlighted in bold in [Supplementary Table 1](#)). These proteins of interest and their synonyms then were entered into a PubMed title/abstract search in association with NASH and its synonyms. This

identified 3 proteins as candidate intermediates for iron-induced adipose tissue dysfunction in NASH. These proteins were adiponectin, annexin A1, and apolipoprotein E (ApoE).

Our SILAC analysis showed that iron treatment resulted in an 81% reduction in annexin A1 secretome signal intensity ($P = .001$). This may be important because annexin A1 knockout (KO) mice show greater degrees of hepatic lobular inflammation and fibrosis than controls when fed a methionine-choline-deficient diet.⁵ Adipocyte iron also previously has been shown to transcriptionally down-regulate serum adiponectin in mouse-derived adipocytes, 3T3-L1 cells.⁶ Our findings now support this in a human adipocyte cell line with a 55% reduction in adiponectin signal intensity in iron-treated SGBS cells ($P = .005$).

We next focused on the iron regulation of ApoE secretion. ApoE appears to protect against steatohepatitis in mice. In an ApoE KO model, unlike wild-type controls, ApoE KO mice fed 7 weeks of a Western diet developed impaired glucose tolerance, steatohepatitis, and hepatic fibrosis.⁷ ApoE is a component of lipoproteins, and promotes very low density lipoprotein-induced adipogenesis.⁸ ApoE knockout mice also readily develop atherosclerosis on an atherogenic diet.⁸

Iron reduced secreted ApoE by 58% ($P = .001$) and 76% ($P = .007$), as

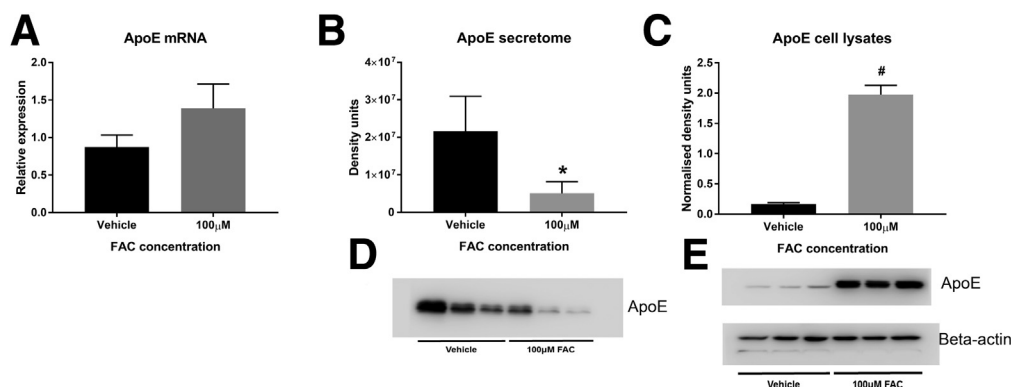


Figure 1. SGBS ApoE expression after FAC treatment. (A) ApoE mRNA ($P = \text{NS}$, ratio paired t test), (B) secretome ApoE densitometry ($*P = .001$, ratio paired t test), (C) lysate ApoE densitometry normalized to β -actin ($\#P = .0005$, ratio paired t test), (D) secretome ApoE immunoblot, and (E) whole-cell lysate ApoE and β -actin immunoblots ($N = 3$ per group). Data are presented as means and SEM.

measured by SILAC and Western blot, respectively. Conversely, iron treatment increased intracellular ApoE levels by more than 11-fold ($P = .0005$), without causing a significant change in mRNA levels (Figure 1). It therefore appears that iron inhibits the secretion of ApoE from adipocytes, causing ApoE to become sequestered intracellularly.

Similar effects on ApoE secretion have been shown with iron treatment in primary cultured astrocytes and cortical neurons.⁹ Taken together with our data, it seems possible that iron may have similar effects on a range of cell types and represents a clear target for further investigation. Treatment with iron in our study showed an up-regulation of anti-oxidant responses (heme-oxygenase-1 and glutathione peroxidase-1 mRNA), indicating the presence of oxidative stress. Interleukin 6 mRNA, however, was not increased with iron treatment, and there was no difference among multiple markers of endoplasmic reticulum stress (Supplementary Figure 3A–I).

We considered whether iron may have a generalized effect on pathways of protein secretion, used by a variety of proteins. We evaluated the role of iron in the secretion of proteins by the classic and exosomal pathways using the UniProt and EVpedia databases, respectively.^{4,10} We found enrichment of signal peptide-containing ($P = .02$), but not exosome-secreted, proteins ($P = .51$) among the iron-dysregulated proteins, suggesting that iron may have a specific effect on proteins secreted via the classic pathway (Supplementary Figure 3J–M).

This research has characterized the effect of iron on the adipocyte secretome. These data provide a platform for multiple avenues for future research. In addition, we have been able to show that increased iron results in sequestration of ApoE within adipocytes, which may be of key importance in the regulation of insulin resistance and liver injury in NASH. Identifying the molecular mechanisms of iron-induced inhibition of ApoE secretion from adipocytes, particularly relating to the role of oxidative stress, may show novel

therapeutic strategies for improving adipocyte function in NASH.

L. J. BRITTON,^{1,2,3,4} KIM BRIDLE,^{1,2}
 LESLEY-ANNE JASKOWSKI,^{1,2}
 JINGJING HE,⁴ CHOAPING NG,^{4,5}
 JAYDE E. RUELCKE,⁶
 AHMED MOHAMED,^{6,7}
 JANSKE REILING,^{1,2,8}
 NISHREEN SANTRAMPURWALA,^{1,2}
 MICHELLE M. HILL,^{6,7}
 JONATHAN P. WHITEHEAD,^{4,5}
 V. NATHAN SUBRAMANIAM,⁹
 DARRELL H. G. CRAWFORD,^{1,2}

¹Gallipoli Medical Research Institute, Greenslopes Private Hospital, Greenslopes, Queensland, Australia

²Faculty of Medicine, The University of Queensland, Herston, Queensland, Australia

³Department of Gastroenterology, Princess Alexandra Hospital, Queensland, Australia

⁴Mater Research, Translational Research Institute, Woolloongabba, Queensland, Australia

⁵School of Life Sciences, University of Lincoln, Lincoln, United Kingdom

⁶The University of Queensland Diamantina Institute, Faculty of Medicine, University of Queensland, Queensland, Australia

⁷QIMR Berghofer Medical Research Institute, Brisbane, Queensland, Australia

⁸Department of Surgery, NUTRIM School of Nutrition and Translational Research in Metabolism, Maastricht University, Maastricht, The Netherlands

⁹Institute of Health and Biomedical Innovation, School of Biomedical Sciences, Queensland University of Technology, Kelvin Grove, Queensland, Australia


Corresponding author: e-mail: l.britton@uq.edu.au.

References

1. Hebbard L, et al. *Nat Rev Gastroenterol Hepatol* 2011;8:35–44.
2. Orr JS, et al. *Diabetes* 2014; 63:421–432.
3. Simcox JA, et al. *Cell Metab* 2013;3:29–341.
4. The UniProt Consortium. *Nucleic Acids Res* 2017;D158–D169.

5. Locatelli I, et al. *Hepatology* 2014; 60:531–544.
6. Gabrielsen JS, et al. *J Clin Invest* 2012;122:3529–3540.
7. Schierwagen R, et al. *Sci Rep* 2015; 5:12931.
8. Pendse AA, et al. *J Lipid Res* 2009; 50:S178–S182.
9. Xu H, et al. *J Alzheimers Dis* 2016; 31:471–487.
10. Kim DK, et al. *Bioinformatics* 2015; 31:933–939.

Abbreviations used in this letter: ApoE, apolipoprotein E; FAC, ferric ammonium citrate; KO, knockout; mRNA, messenger RNA; NASH, nonalcoholic steatohepatitis; SGBS, Simpson-Golabi-Behmel Syndrome; SILAC, stable isotope labeled amino acids in cell culture.

 Most current article

© 2018 The Authors. Published by Elsevier Inc. on behalf of the AGA Institute. This is an open access article under the CC BY-NC-ND license (<http://creativecommons.org/licenses/by-nc-nd/4.0/>).

2352-345X

<https://doi.org/10.1016/j.jcmgh.2018.04.005>

Received December 21, 2017. Accepted April 2, 2018.

Acknowledgment

ProteomeXchange Consortium via the Proteomics Identifications (PRIDE) partner repository: <http://proteomecentral.proteomexchange.org/cgi/GetDataset?ID=pxd006341> data set identifier PXD006341.

Author contributions

L. J. Britton was responsible for the study concept and design, acquisition of data, analysis and interpretation of data, drafting of the manuscript, and statistical analysis; K. Bridle was responsible for the study concept and design, analysis and interpretation of data, critical revision of the manuscript for important intellectual content, administrative, technical, or material support, and study supervision; L. A. Jaskowski was responsible for the acquisition of data, analysis and interpretation of data, critical revision of the manuscript for important intellectual content, and administrative, technical, or material support; J. He was responsible for the acquisition of data, critical revision of the manuscript for important intellectual content, and administrative, technical, or material support; C. Ng was responsible for the acquisition of data, critical revision of the manuscript for important intellectual content, and administrative, technical, or material support; J. E. Ruelcke was responsible for the acquisition of data, analysis and interpretation of data, critical revision of the manuscript for important intellectual content, statistical analysis, and administrative, technical, or material support; A. Mohamed was responsible for the analysis and interpretation of data, critical revision of the manuscript for important intellectual content, and statistical analysis; J. Reiling was responsible for the study concept and design, analysis and

interpretation of data, and critical revision of the manuscript for important intellectual content; N. Santrampurwala was responsible for the study concept and design, analysis and interpretation of data, and critical revision of the manuscript for important intellectual content; M. M. Hill was responsible for the study concept and design, analysis and interpretation of data, critical revision of the manuscript for important intellectual content, statistical analysis, administrative, technical, or material support, and study supervision; J. P.

Whitehead was responsible for the study concept and design, analysis and interpretation of data, critical revision of the manuscript for important intellectual content, administrative, technical, or material support, and study supervision; V. N. Subramaniam was responsible for the study concept and design and critical revision of the manuscript for important intellectual content; and D. H. G. Crawford was responsible for the study concept and design, analysis and interpretation of data, critical revision of the manuscript for

important intellectual content, obtained funding, administrative, technical, or material support, and study supervision.

Conflicts of interest

The authors disclose no conflicts.

Funding

This research was supported by Australian National Health and Medical Research Council grant APP1029574.

Supplementary Methods

Simpson-Golabi-Behmel Syndrome Pre-Adipocyte Differentiation and Iron Treatment

SGBS pre-adipocytes were a gift from Martin Wabitsch (University of Ulm, Ulm, Germany).^{1,2} SGBS cells were passaged, proliferated, and differentiated at less than 50 generations in 12-well plates and 100-mm dishes as previously described.³ Cells were treated with 90 $\mu\text{g}/\text{mL}$ heparin and 1 ng/mL fibroblast growth factor-1 (both Sigma-Aldrich, St. Louis, MO) throughout proliferation and differentiation. After 14 days of differentiation, cells were incubated with 0, 25, 100, or 500 $\mu\text{mol}/\text{L}$ FAC (Sigma-Aldrich) for 24 hours. Media then was replaced with the same for a further 24 hours until the end of the experiment.

RNA Extraction and Real-Time Quantitative Polymerase Chain Reaction

RNA was extracted from treated SGBS adipocytes using a PureLink RNA mini kit (Invitrogen, Carlsbad, CA). Complementary DNA was synthesized from 1 μg RNA using a Sensifast complementary DNA synthesis kit (Bioline, London, UK) after treatment with DNase 1 (Invitrogen). Samples underwent thermal cycling using a ViiA7 real-time polymerase chain reaction machine (Invitrogen) with a Sensifast SYBR Lo-ROX Kit (Bioline). The following protocol was used: 2 minutes at 95°C, then 40 cycles of 5 seconds at 95°C, alternating with 20 seconds at 63°C, followed by a melt curve analysis. Relative mRNA quantities were determined by calibration of cycle threshold values to the standard curve of pooled complementary DNA samples. Results were normalized to cycle threshold values of cyclophilin.

Iron, Cellular Viability (MTS), and Protein Assays

Iron levels were quantified using a chromagen reagent method.⁴ Cellular viability was assessed using a CellTiter 96 Aqueous One Solution Cell Proliferation Assay (Promega, Madison, WI)

according to the manufacturer's instructions. Whole-cell lysate and secretome samples underwent protein estimation using a Pierce BCA protein assay kit (Thermo Fisher Scientific, Waltham, MA).

Stable Isotope-Labeled Amino Acids in Cell Culture Proteomics

SILAC incorporates stable amino acid isotopes, without altering cellular biology, allowing direct comparison of the secretome by mass spectrometry between treatment groups.⁵ SGBS pre-adipocytes were grown in SILAC Dulbecco's modified Eagle medium:F12 media (Thermo Fisher Scientific) supplemented with dialyzed fetal bovine serum (Thermo Fisher Scientific) and 22.81 mg/L $^2\text{H}_4$ -lysine and 36.88 mg/L $^{13}\text{C}_6$ -arginine (K4R6) or 22.81 mg/L $^{13}\text{C}_6$ $^{15}\text{N}_2$ -lysine and 36.88 mg/L $^{13}\text{C}_6$ $^{15}\text{N}_4$ -arginine (K8R10). Incorporation of labeled amino acids was confirmed by liquid chromatography tandem mass spectrometry on tryptic peptides prepared from whole-cell lysates. Cell pellets were lysed in 8 mol/L urea in 100 mmol/L triethylammonium bicarbonate, and protein concentration was estimated using the Bradford assay (BioRad, Hercules, CA). Thirty micrograms of cell lysate was reduced and alkylated by incubating samples for 30 minutes at 37°C with 2.5 mmol/L tris(2-carboxyethyl) phosphine and then 5 mmol/L 2-chloroacetamide. The urea concentration was diluted to 1 mol/L with 100 mmol/L triethylammonium bicarbonate before adding 0.6 μg of trypsin. Samples were incubated overnight then acidified to 1% trifluoroacetic acid and cleaned with OMIX C18 tips according to the manufacturers' protocol (Agilent, Santa Clara, CA). Liquid chromatography tandem mass spectrometry was performed as described later.

Labeled (>97%) cells underwent differentiation to adipocytes as described earlier. At day 14 after differentiation, cells were treated with vehicle (media) (K4R6, medium-weight cells) or 100 $\mu\text{mol}/\text{L}$ FAC (in media) (K8R10, heavy-weight cells) for a further 48 hours using exactly

equal volumes of media, replacing the media after 24 hours. Media for secretome analysis was collected from K4R6 and K8R10 cells and mixed 1:1 (vol/vol) before centrifugation at 600 \times g at 4°C for 10 minutes to remove cell debris. Supernatant then was concentrated using Amicon Ultra 15 mL 10-kilodalton centrifugal filter units (Merck Millipore, Burlington, MA) in a fixed-angle centrifuge at 5000 \times g to provide approximately 1-mL samples of concentrated mixed secretome. Thirty micrograms of protein was separated on 10% sodium dodecyl sulfate-polyacrylamide electrophoresis gels to 10 mm. Protein visualization, excision of bands, and in-gel trypsin digestion were performed using a semiautomated method as described.⁶ A band corresponding to the same molecular weight as transferrin (media additive) was removed before digestion to provide a protein sample exclusively secreted from cultured adipocytes.

Mass Spectrometry

A Q Exactive Plus Orbitrap Mass Spectrometer (Thermo Fisher Scientific), coupled with Easy-nLC 1000 and EASY-spray ion source (both Thermo Fisher Scientific), was used to analyze the digested peptides. Samples were loaded onto an EASY-Spray PepMap RSLC C18 2- μm column (50 cm \times 75 μm ID), with a Nanoviper Acclaim C18 guard (75 μm \times 2 cm) (both Thermo Fisher Scientific). A 90-minute method was run using a combination of buffer A (0.1% formic acid) and buffer B (0.1% formic acid:acetonitrile). A 2-step gradient was run comprising a 60-minute gradient from 3% to 25% buffer B and a 12-minute gradient from 25% to 40% buffer B. The flow rate was 250 nL/min. The mass spectrometer was programmed to acquire a full mass spectrometry resolution of 70,000 with an ACG target of 3×10^6 , with a maximum injection time of 100 ms. The mass spectrometry scan range was from 350 to 1400 m/z. Tandem mass spectrometry was set to acquire a resolution of 17,500 with an ACG target of 5×10^5 and a maximum injection time of 55 ms. The loop

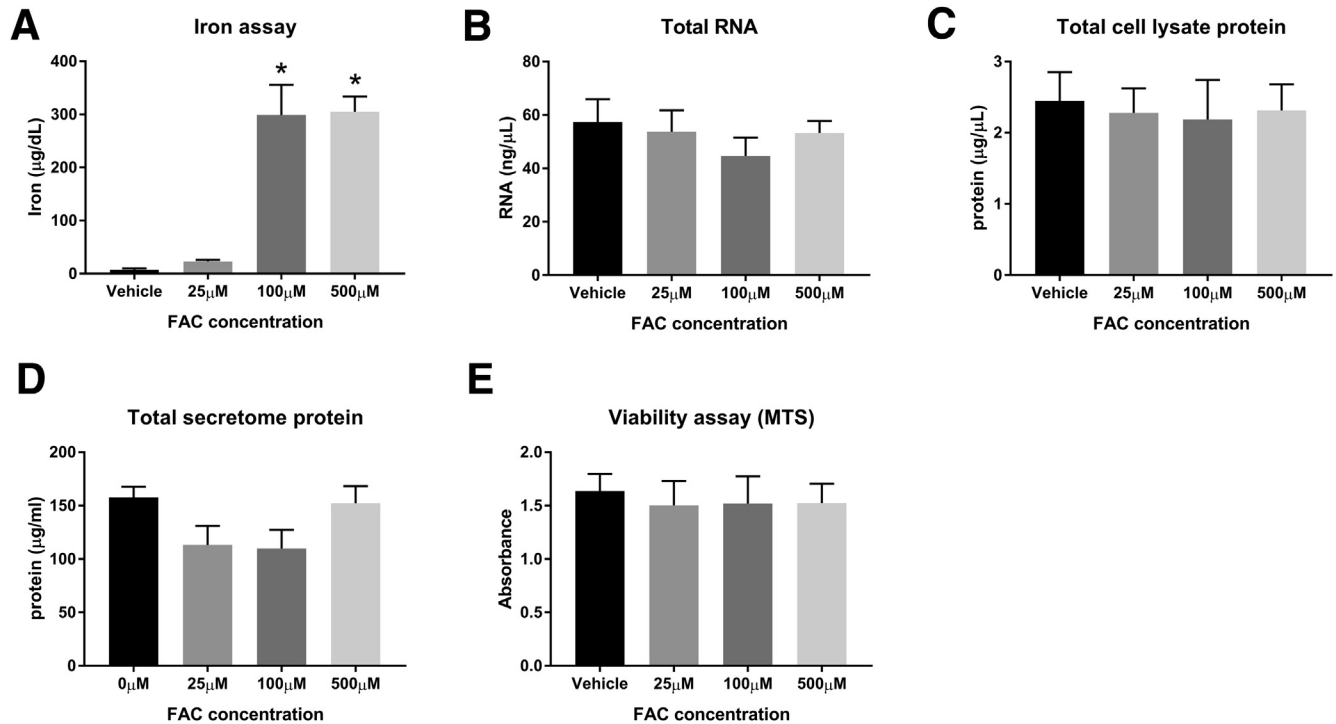
count was set to 20 with a dynamic exclusion after 30 seconds. Raw data were processed with Spectrum mill (Rev B.05.00.181 SP1; Agilent). Selected modifications included fixed carbamidomethylation of cysteine and SILAC labels (Arg 0-6-10 daltons Lys 0-4-8 daltons) and variable oxidized methionine. Results were searched against the Human UniProt database (downloaded June 1, 2015).⁷ Trypsin was selected as the digestion enzyme, with 2 maximum missed cleavages allowed. The precursor mass tolerance was set at ± 20 ppm and product mass tolerance was ± 20 ppm. Data were analyzed using the online Quantitative Proteomics *P* value Calculator using no normalization and nonadjusted *P* values.⁸

Immunoblotting

Western blot using whole-cell lysate samples (10 μ g) and 5- μ L concentrated secretome samples was performed as previously described.⁹ A 1:500 dilution of primary antibody against ApoE (sc-53570; Santa Cruz, Dallas, TX) was applied to the membranes. A 1:100,000 dilution of goat anti-mouse horseradish peroxidase antibody (Invitrogen) was applied as secondary antibody. ApoE whole-cell lysate densitometry was normalized against densitometry using β -actin as a reference protein (1:2000 primary antibody) (cat no. 4967, Cell Signaling, Danvers, MA) and 1:20,000 goat anti-rabbit horseradish-peroxidase antibody (Invitrogen).

References

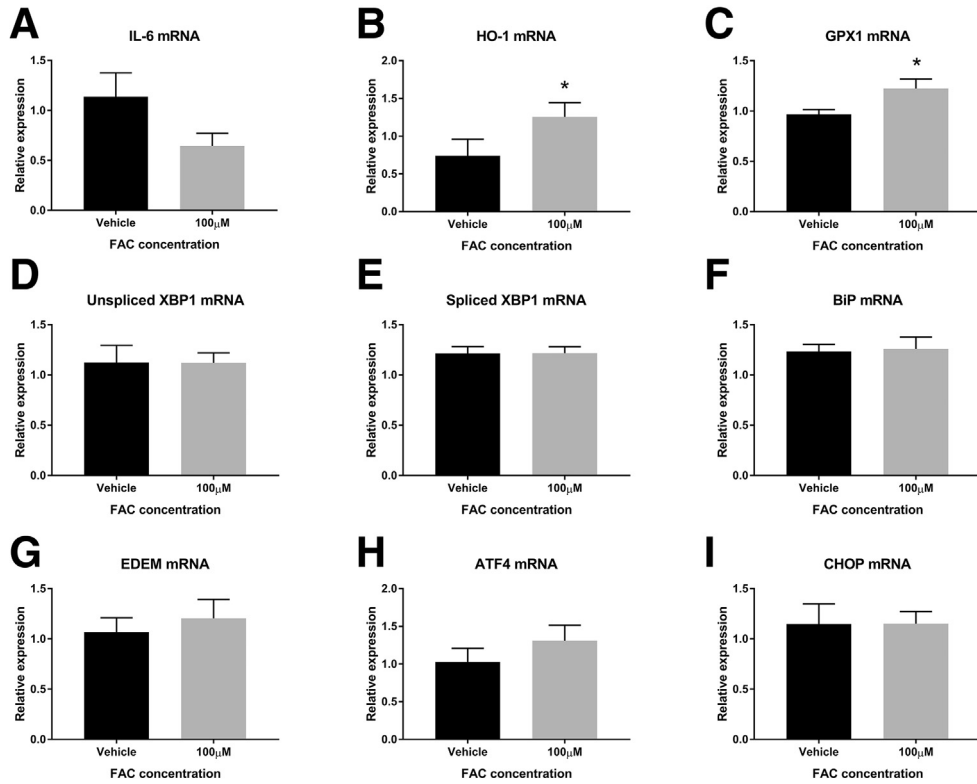
1. Wabitsch M, et al. *Int J Obes Relat Metab Disord* 2001;25:8–15.
2. Fischer-Posovszky P, et al. *Obes Facts* 2008;184–189.
3. Luo X, et al. *Diabetes* 2012; 61:124–136.
4. Kohyama M, et al. *Nature* 2009; 457:318–321.
5. Ong SE, et al. *Nat Protoc* 2006; 1:2650–2660.
6. Ruelcke JE, et al. *J Proteomics* 2016;149:3–6.
7. The UniProt C. *Nucleic Acids Res* 2017;D158–D169.
8. Chen D, et al. *J Proteome Res* 2014;13:4184–4191.
9. Britton L, et al. *Physiol Rep* 2016:e12837.



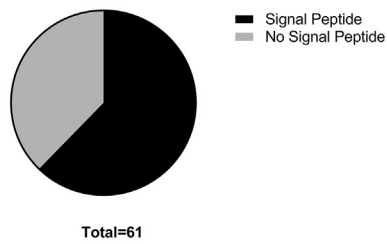
Supplementary Figure 1. Optimization of iron loading in SGBS cells. (A) Iron assay, $P = .004$ (1-way analysis of variance [ANOVA]), $*P < .01$ (Dunnett multiple comparisons test compared with $0 \mu\text{mol/L}$ FAC, $n = 2$ per group). (B) Total RNA ($P = \text{NS}$ by 1-way ANOVA, $N = 3$ per group). (C) Total lysate protein ($P = \text{NS}$ by 1-way ANOVA, $n = 3$ per group). (D) Total secretome protein ($P = \text{NS}$ by 1-way ANOVA, $N = 3$ per group). (E) Viability assay (MTS) ($P = \text{NS}$ by 1-way ANOVA, $N = 3$ per group). Data are presented as means and SEM. MTS, [3-(4,5-dimethylthiazol-2-yl)-5-(3-carboxymethoxyphenyl)-2-(4-sulfophenyl)-2H-tetrazolium].



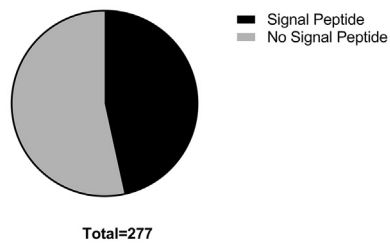
Supplementary Figure 2. Volcano plot of relative signal intensity of proteins identified in the adipocyte secretome. The x-axis denotes \log_2 of the ratio of iron/vehicle-treated cells, with proteins to the *left* of zero representing those down-regulated by iron and those to the *right* representing up-regulation by iron. The y-axis denotes statistical significance with a *line* representing a P value of .05. Proteins above this *line* have a P value $< .05$. SILAC-labeled adipocytes generated 338 proteins that were identified in the secretome by mass spectrometry. Of these, 213 had reduced signal intensity in response to iron, whereas 125 had increased signal intensity. Of the 213 proteins with reduced signal intensity, 61 had a statistically significant ($P < .05$) down-regulation in response to iron. Of these, 53 had a greater than 2-fold decrease in response to iron. Of the 125 proteins with increased signal intensity, 11 had a statistically significant ($P < .05$) up-regulation in response to iron. Of these, 7 proteins had a greater than 2-fold increase response to iron. Those proteins containing signal peptide (as determined by signal peptide annotations on the UniProt database) are shown in red. Those without signal peptide are shown in blue.



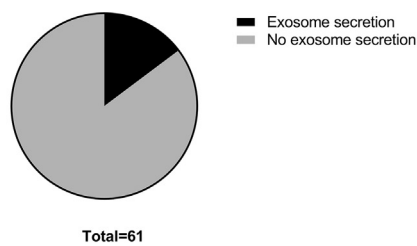
J Significantly down-regulated proteins



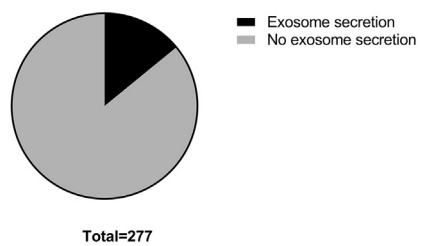
K Not significantly down-regulated proteins



L Significantly down-regulated proteins



M Not significantly down-regulated proteins



Supplementary Figure 3. (See previous page). Mechanistic aspects of iron-related dysregulation of protein secretion.

(A) Interleukin 6 (IL6) mRNA ($P = \text{NS}$, paired t test, $N = 3$ per group). (B and C) Oxidative stress ($*P < .05$, both $N = 3$ per group). (B) Heme-oxygenase (HO-1) mRNA ($P = .01$, paired t test). (C) Glutathione peroxidase 1 (GPX1) mRNA ($P = .049$, paired t test). (D–I) Endoplasmic reticulum stress (all $N = 3$ per group). (D) Unspliced X-box binding protein (XBP1) mRNA ($P = \text{NS}$, paired t test). (E) Spliced XBP1 mRNA ($P = \text{NS}$, paired t test). (F) Immunoglobulin binding protein (BiP) mRNA ($P = \text{NS}$, paired t test). (G) Endoplasmic reticulum degradation-enhancing α -mannidose-like protein (EDEM) mRNA ($P = \text{NS}$, paired t test). (H) Activating transcription factor 4 (ATF4) mRNA ($P = \text{NS}$, paired t test). (I) CCAAT/enhancer-binding protein homologous protein (CHOP) mRNA ($P = \text{NS}$, paired t test). (J–M) Enrichment with signal peptide and exosome proteins. (J) Proportion of proteins down-regulated significantly by iron with signal peptide vs no signal peptide. (K) Proportion of proteins not down-regulated significantly by iron with signal peptide vs no signal peptide. (L) Proportion of proteins down-regulated significantly by iron with exosome secretion vs no exosome secretion. (M) Proportion of proteins not down-regulated significantly by iron with exosome secretion vs no exosome secretion. Of the 61 proteins down-regulated significantly, 62% (38 of 61) had signal peptide, whereas of the remaining proteins only 47% (129 of 277) had signal peptide. The 1-tailed Fisher exact test showed significant enrichment with signal peptide ($P = .02$) among the group down-regulated significantly. In contrast, there was no significant enrichment of the exosomal pathway ($P = .51$, 1-tailed Fisher exact test), because 15% (9 of 61) of the proteins down-regulated significantly and 14% (39 of 277) of the remaining secretome proteins had been reported previously in the high-confidence proteins from the EVpedia database.

Supplementary Table 1.List of SGBS Secretome Proteins With Significantly Altered Signal Intensity in Response to Iron

Accession number	Gene name	Protein name	Mean signal intensity ratio, iron/vehicle	SD	P value
Q8IX30	SCUBE3	Signal peptide, CUB and EGF-like domain-containing protein 3	0.026	0.016	.001
P61353	RPL27	60S ribosomal protein L27	0.060	0.005	.001
Q9NQH7	XPNPEP3	Probable Xaa-Pro aminopeptidase 3	0.076	0.004	.001
P07996	THBS1	Thrombospondin-1	0.083	0.047	.001
Q76M96	CCDC80	Coiled-coil domain-containing protein 80	0.090	0.031	.001
P78539	SRPX	Sushi repeat-containing protein SRPX	0.096	0.620	.001
Q9UHI8	ADAMTS1	A disintegrin and metalloproteinase with thrombospondin motifs 1	0.114	0.090	.002
Q92538	GBF1	Golgi-specific brefeldin A-resistance guanine nucleotide exchange factor 1	0.118	0.024	.004
Q15063	POSTN	Periostin	0.121	0.149	.001
P08238	HSP90AB1	Heat shock protein (HSP) 90- β	0.125	0.038	.004
P24593	IGFBP5	Insulin-like growth factor-binding protein 5	0.154	0.069	.001
Q15113	PCOLCE	Procollagen C-endopeptidase enhancer 1	0.155	0.088	.001
Q9NTX5	ECHDC1	Ethylmalonyl-CoA decarboxylase	0.158	0.068	.001
P25788	PSMA3	Proteasome subunit α type 3	0.176	0.442	.001
Q12931	TRAP1	Heat shock protein 75 kilodaltons, mitochondrial	0.186	0.028	.018
P04083	ANXA1	Annexin A1	0.192	0.049	.001
P30101	PDIA3	Protein disulfide-isomerase A3	0.198	0.059	.001
Q99985	SEMA3C	Semaphorin-3C	0.199	0.225	.001
Q6NZI2	PTRF	Polymerase I and transcript release factor	0.210	0.134	.001
Q8TAV4	STOML3	Stomatin-like protein 3	0.220	0.084	.006
Q9UKZ9	PCOLCE2	Procollagen C-endopeptidase enhancer 2	0.226	0.030	.001
Q05469	LIPE	Hormone-sensitive lipase	0.231	0.196	.023
Q13642	FHL1	Four and a half LIM domains protein 1	0.263	0.006	.029
P02749	APOH	β 2-glycoprotein 1	0.286	0.310	.048
P02462	COL4A1	Collagen α -1(IV) chain	0.286	0.351	.001
P15311	EZR	Ezrin	0.296	0.077	.003
P42765	ACAA2	3-Ketoacyl-CoA thiolase, mitochondrial	0.308	0.136	.001
P68104	EEF1A1	Elongation factor 1-α 1	0.309	0.215	.001
Q9NQC3	RTN4	Reticulon-4	0.312	0.119	.007
Q8IY17	PNPLA6	Neuropathy target esterase	0.316	0.028	.026
Q92743	HTRA1	Serine protease HTRA1	0.324	0.075	.001
P08294	SOD3	Extracellular superoxide dismutase (Cu-Zn)	0.339	0.027	.005
Q16836	HADH	Hydroxyacyl-coenzyme A dehydrogenase, mitochondrial	0.348	0.207	.011
Q99715	COL12A1	Collagen α -1(XII) chain	0.348	0.183	.001
P07355	ANXA2	Annexin A2	0.354	0.111	.001
P26038	MSN	Moesin	0.362	0.110	.034
P23284	PPIB	Peptidyl-prolyl cis-trans isomerase B	0.374	0.122	.001
O94769	ECM2	Extracellular matrix protein 2	0.375	0.060	.005
Q9NRN5	OLFML3	Olfactomedin-like protein 3	0.389	0.066	.002
P53396	ACLY	Adenosine triphosphate-citrate synthase	0.389	0.066	.001
Q16363	LAMA4	Laminin subunit α -4	0.407	0.091	.001
P14625	HSP90B1	Endoplasmin	0.414	0.068	.025
Q9BU40	CHRDL1	Chordin-like protein 1	0.419	0.264	.001
P02649	APOE	Apolipoprotein E	0.421	0.053	.001
Q9NS98	SEMA3G	Semaphorin-3G	0.425	0.161	.001
P02751	FN1	Fibronectin	0.441	0.146	.001
P14543	NID1	Nidogen-1	0.442	0.190	.006

Supplementary Table 1. Continued

Accession number	Gene name	Protein name	Mean signal intensity ratio, iron/vehicle	SD	<i>P</i> value
Q08431	MFGE8	Lactadherin	0.446	0.167	.026
Q15848	ADIPOQ	Adiponectin	0.449	0.652	.005
O75390	CS	Citrate synthase, mitochondrial	0.454	0.183	.012
Q92626	PXDN	Peroxidasin homolog	0.457	0.200	.001
P07942	LAMB1	Laminin subunit β 1	0.484	0.110	.001
Q08629	SPOCK1	Testican-1	0.497	0.055	.014
O00462	MANBA	β -mannosidase	2.180	2.560	.034
Q13510	ASAH1	Acid ceramidase	2.222	3.135	.048
P02794	FTH1	Ferritin heavy chain	2.451	0.769	.030
Q02952	AKAP12	A-kinase anchor protein 12	2.665	0.572	.047
A6NCN2	KRT87P	Putative keratin-87 protein	4.113	0.011	.022
P23468	PTPRD	Receptor-type tyrosine-protein phosphatase δ	10.687	2.199	.003
P10586	PTPRF	Receptor-type tyrosine-protein phosphatase F	11.935	3.955	.001

NOTE. Proteins shown had a greater than 2-fold change in signal intensity in response to iron, with $P < .05$. Proteins highlighted in bold represent the 20 proteins of interest after review of the UniProt protein descriptions. Data were analyzed using the online Quantitative Proteomics *P* value Calculator using no normalization and nonadjusted *P* values ($N = 3$ per group). CUB, C1r/C1s, Uegf, bone morphogenetic protein-1; EGF, epidermal growth factor; HTRA, High-Temperature Requirement A.